ARMY RESEARCH LABORATORY

Ballistic Effects of Ignition Stimulus in High-Performance Tank Ammunition

Lang-Mann Chang

ARL-TR-1092 May 1996

NOTICES

Destroy this report when it is no longer needed. DO NOT return it to the originator.

Additional copies of this report may be obtained from the National Technical Information Service, U.S. Department of Commerce, 5285 Port Royal Road, Springfield, VA 22161.

The findings of this report are not to be construed as an official Department of the Army position, unless so designated by other authorized documents.

The use of trade names or manufacturers' names in this report does not constitute indorsement of any commercial product.

REPORT DOCUMENTATION PAGE

Form Approved
OMB No. 0704-0188

1. AGENCY USE ONLY *(Leave blank)*	2. REPORT DATE	3. REPORT TYPE AND DATES COVERED
	May 1996	Final, Feb 94 - Sep 95

4. TITLE AND SUBTITLE

Ballistic Effects of Ignition Stimulus in High-Performance Tank Ammunition

5. FUNDING NUMBERS

PR: 1L162618AH80

6. AUTHOR(S)

Lang-Mann Chang

7. PERFORMING ORGANIZATION NAME(S) AND ADDRESS(ES)

U.S. Army Research Laboratory
ATTN: AMSRL-WT-PA
Aberdeen Proving Ground, MD 21005-5066

8. PERFORMING ORGANIZATION REPORT NUMBER

ARL-TR-1092

9. SPONSORING/MONITORING AGENCY NAME(S) AND ADDRESS(ES)

10. SPONSORING/MONITORING AGENCY REPORT NUMBER

11. SUPPLEMENTARY NOTES

12a. DISTRIBUTION/AVAILABILITY STATEMENT

Approved for public release; distribution is unlimited.

12b. DISTRIBUTION CODE

13. ABSTRACT *(Maximum 200 words)*

Ballistic effects of ignition stimulus in a high-performance tank propelling charge are studied through the use of a two-phase flow computer code, XKTC. The studies are conducted with an array of generic igniters that have output rates that vary along the charge length. Performance evaluations of the igniters are based on their resultant pressure behavior in the gun chamber, muzzle velocity, intergranular stress level, and other related variables. Results provide guidelines for the design of effective igniters for granular propelling charges. Details of ignition dynamics as well as their correlations with ballistic performance are explained.

14. SUBJECT TERMS

ignition stimulus; igniters; ballistic simulation; intergranular stress

15. NUMBER OF PAGES

30

16. PRICE CODE

17. SECURITY CLASSIFICATION OF REPORT	18. SECURITY CLASSIFICATION OF THIS PAGE	19. SECURITY CLASSIFICATION OF ABSTRACT	20. LIMITATION OF ABSTRACT
UNCLASSIFIED	UNCLASSIFIED	UNCLASSIFIED	UL

INTENTIONALLY LEFT BLANK.

ACKNOWLEDGMENTS

The author wishes to thank Mr. Ronald D. Anderson, U.S. Army Research Laboratory, for his assistance in using the SiliconGraphics machine to obtain the graphics for the flamespreading.

INTENTIONALLY LEFT BLANK.

TABLE OF CONTENTS

		Page
	LIST OF FIGURES	vii
	LIST OF TABLES	vii
1.	INTRODUCTION	1
2.	DESCRIPTION OF IGNITERS	2
3.	MODELING	4
3.1	Geometrical Representation of the Gun Chamber	4
3.2	Input Data	4
4.	RESULTS AND DISCUSSION	5
4.1	Ballistic Validation of the Computer Code With Firing Data.	5
4.2	Effects of Igniter Output Distribution	6
4.3	Effects of Igniter Output Rate	16
4.4	Correlations of Muzzle Velocity Increase (ΔV_m), Intergranular Stress (S_i), and Maximum Breech Pressure (P_b) With Negative Pressure Difference ($-\Delta P$)	17
5.	CONCLUSIONS	17
6.	REFERENCE	21
	DISTRIBUTION LIST	23

INTENTIONALLY LEFT BLANK.

LIST OF FIGURES

Figure — Page

1. Typical pressure waves 1
2. Igniter configurations 3
3. Pressure data for Baseline Igniter 6
4. Pressure data for Igniter A 7
5. Pressure data for Igniter B 9
6. Pressure data and projectile travel for Igniter C 9
7. Flamespreading (FS), grain velocity (V), and intergranular stress (S_i) for Igniter C 10
8. Pressure data for Igniter D 11
9. Pressure data for Igniter E 12
10. Flamespreading (FS), grain velocity (V), and intergranular stress (S_i) for Igniter E 12
11. Pressure data for Igniter F 13
12. Pressure data for Igniter G 14
13. Flamespread in gun chamber for Igniter H (at 2 ms) 14
14. Increased igniter output rate of Igniter H 15
15. Pressure data for Igniter H (total mass of igniter output = 30 g and 75.5 g) 15
16. Pressure data for Igniter H (total mass of igniter output = 30 g; total output time = 1.5 ms and 3 ms) 16
17. Correlations of Muzzle Velocity Increase (ΔV_m), Intergranular Stress (S_i), and Maximum Breech Pessure (P_b) With Negative Pressure Difference ($-\Delta P$) 18

LIST OF TABLES

Table — Page

1. Constants for Burn Rate 5
2. Summary of Calculated Results 8

INTENTIONALLY LEFT BLANK.

1. INTRODUCTION

The ever-increasing demand for enhanced performance of tank gun systems usually requires increased charge loading density, or increased chemical energy of propellant, or a combination of both. However, severe pressure wave problems are often encountered, especially when nonconventional propellant formulations and granulations are involved. In fact, pressure waves have been implicated in the catastrophic overpressure of several artillery and tank cannons (Horst 1986; May and Horst 1978). Figure 1 shows typical high-amplititude pressure waves occuring in gun firings (Horst 1986). Most of the incidents have been determined to be caused by improper ignition stimulus. Although gun simulator studies have been very successful in elucidating many insights into the ignition phenomena (Chang and Rocchio 1988; Minor 1983), many other important parts of the ignition dynamics and their ballistic effects are difficult to determine merely by experiments. Using experimentally measured igniter output, however, computer simulations can provide the needed information for facilitating charge development and ensuring the required performance of the ammunition, as well as for safety precautions.

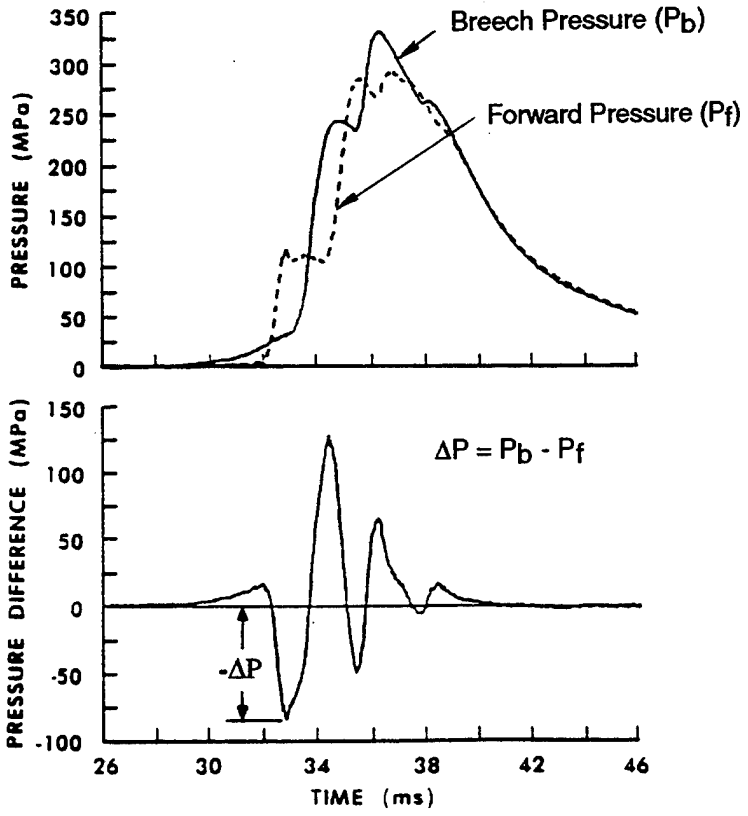

Figure 1. Typical pressure waves.

In this work, we study the ballistic effects of an array of generic igniters for ignition of a granular tank propelling charge. The ignition stimulus provided by the igniters is allowed to vary with time and location along the charge length. The performance of the individual igniter is evaluated based on its resultant pressure-time profile in the gun chamber, muzzle velocity, intergranular stress level, and other related variables.

The ballistic simulations are performed by employing the two-phase flow interior ballistic code XKTC (Gough 1990). Of its many features, the capabilities of allowing the igniter output to vary with time and location and accounting for projectile intrusion into the propellant bed are particularly important in this application.

2. DESCRIPTION OF IGNITERS

Several generic igniters are considered in this study, along with a baseline igniter for performance comparison. These are sketched in Figure 2 and are described as follows.

Baseline Igniter. This is the igniter for which gun firing data are available. It is a typical bayonet-type metal primer, allowing a maximum loading of 1.29 g of benite strands. As depicted in Figure 2, the primer has a blank segment near the primer headstock and has a venting tip. (Note: the wide black line in Figure 2 represents the length of the combustion chamber)

Igniter A. This igniter resembles the baseline igniter, but with uniform venting along the whole length.

Igniter B. This igniter is simply an extension of Igniter A to cover the full length of the propelling charge.

Igniter C. This is a basepad igniter whose output is confined in a narrow region (e.g., 12.5 mm wide) at the rear end of the propelling charge to represent an extreme of localized output.

Igniter D. This represents another extreme of localized output, with the ignition source confined at the forward end of the propelling charge.

Igniter E. This igniter represents the case of a confined igniter output located at the midsection of the propelling charge.

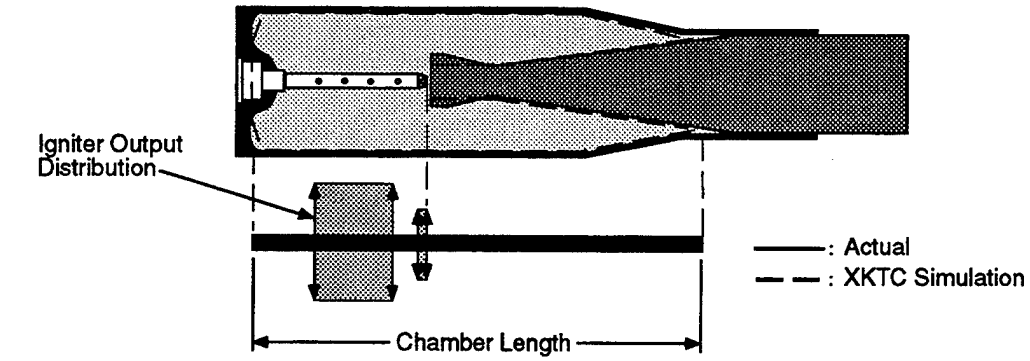

Baseline Igniter

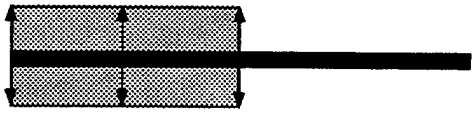

Igniter A

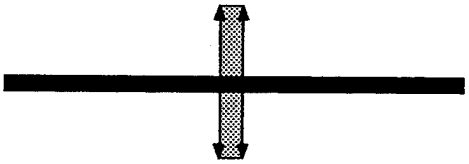

Igniter E

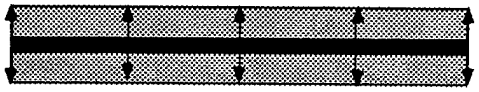

Igniter B

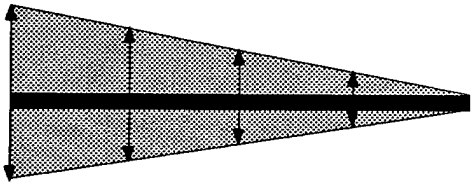

Igniter F

Igniter C

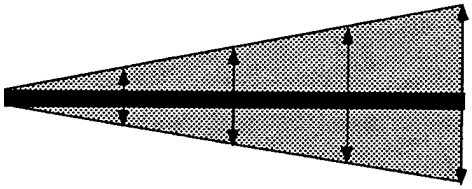

Igniter G

Igniter D

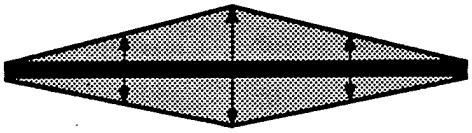

Igniter H

Figure 2. Igniter configurations.

Igniter F. This igniter assumes a wedge-shaped output profile, with output decreasing linearly to zero from the rear to the forward end of the propelling charge.

Igniter G. As a reverse of Igniter F, the output increases linearly toward the forward end of the propelling charge.

Igniter H. The output rate of this igniter decreases linearly from its maximum at the mid section to zero at the two ends of the propelling charge.

3. MODELING

The following section discusses the geometric representation of the gun chamber suitable for the XKTC code and some of the primary input data for the code.

3.1 Geometrical Representation of the Gun Chamber.

The gun system being considered is a 105-mm tank gun. The gun chamber referred to hereafter is the chamber inside the steel cartridge case. To conform to the one-dimensional XKTC code, the projectile assembly is compressed to a solid cylinder that maintains the same volume. The top of Figure 2 shows both the actual (solid line) and the XKTC (dashed line) representations of the gun chamber.

3.2 Input Data.

Presented in the following paragraphs are some of the major input data for the XKTC code.

Propellant. The propellant considered is a nitramine composite formulation, with a cylindrical grain geometry of 8.33 mm in diameter and 14.12 mm long, and each grain has seven perforations. Based on data from closed bombs and strand burner tests, the burn rates of the propellant can suitably be represented by a curve composed of three segments, where each segment is in the form of

$$\text{Burn Rate (mm/s)} = aP^b,$$

and where a and b are constants and P is pressure in Megapascals (MPa). The values of a and b for the three segments are given in Table 1.

Table 1. Constants for Burn Rate

Pressure Range (MPa)	a	b
0 - 48	1.7807	0.85090
48 - 138	5.9420	0.540194
greater than 138	1.1010	0.8699

Gun Bore Resistance Profile. The bore resistance to projectile motion is particularly large during the engraving period of the obturator, which occurs in the first few centimeters of projectile travel. After that, the resistance falls rapidly along the gun tube. In practice, the bore resistance is extremely difficult to measure accurately. Lacking experiment data, however, it can be approximated by iteratively adjusting the resistance profile until both the calculated chamber pressure and the projectile velocity at the muzzle satisfactorily match firing data. The bore resistance determined can then be used for ballistic analysis of other charges fired from the same gun system. It is noted that the resistance attributable to the air pressure building up in front of the moving projectile can be calculated in the code and was included in this study.

Igniter Output. To establish a common ground for performance comparison, we consider that all igniters contain the same mass of identical energetic material to ensure same energy output. Since the baseline igniter contains 30 g of benite, we assume that all igniters contain the same mass of igniter material, unless indicated otherwise. Additionally, we specify the effective output time of each igniter to be 3 ms, during which a benite igniter has significant venting, although the venting could last as long as 40 ms (Chang and Rocchio 1988). For the purpose of examining effects of output rate, we also consider a case of reducing the output from 3 ms to 1.5 ms.

4. RESULTS AND DISCUSSION

4.1 Ballistic Validation of the Computer Code With Firing Data.

A simulation is first performed with the subject propelling charge using the baseline igniter to match test data. The calculated maximum chamber pressure, 507 MPa, at 362 mm from the breech face is in good agrement with the firing data of 506.7 MPa averaged from five rounds in the test series. The calculated projectile velocity at the muzzle is only 1 m/s lower than the actual firing result. This simulation calibrates the computer code by determining the bore resistance profile as

explained earlier. Moreover, the calculated results serve as a baseline for performance comparison of the igniters being evaluated. Figure 3 shows the calculated pressures at the breech and at the forward end of the gun chamber and their differential. Note that the times indicated are referred to the instant that the igniter output begins.

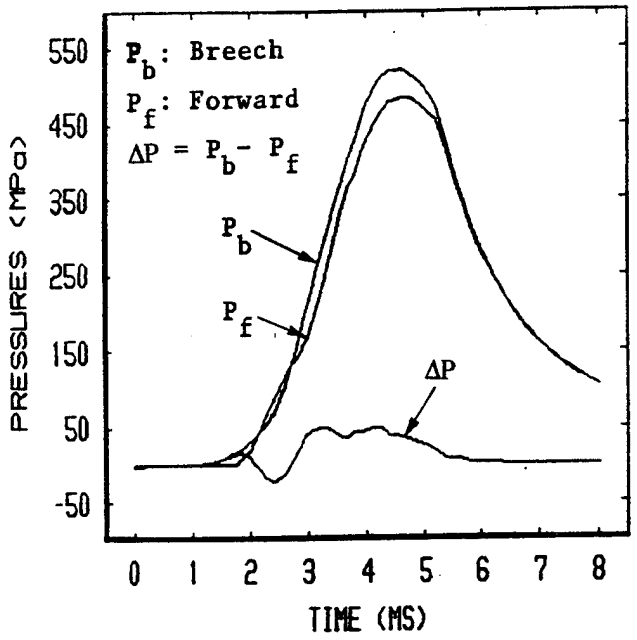

Figure 3. Pressure data for Baseline Igniter.

4.2 Effects of Igniter Output Distribution.

In the examination of the ballistic effects of the various igniters, particular emphasis will be placed on the behavior of gun chamber pressure because of the concern of safety. For simplicity, we designate P_b = breech pressure , P_f = forward pressure, and $\Delta P = P_b - P_f$. Desired pressure behavior is characterized by smooth pressure-time curves at the two ends of the gun chamber and a minimum negative difference ($-\Delta P$) of the two pressures. The intergranular stress in the propellant bed, the muzzle velocity, and ignition delay time are also factors to be considered. Table 2 summarizes all calculated results for the igniters studied.

Igniter A. Figure 4 illustrates the chamber pressure behavior, which can be compared to the baseline configuration in Figure 3. Igniter A shows some improvement over the baseline igniter with smoother pressure-time curves and a smaller value of $-\Delta P$. The muzzle velocity has a small increase of 8 m/s, and the intergranular stress S_i is slightly decreased (as noted in the table).

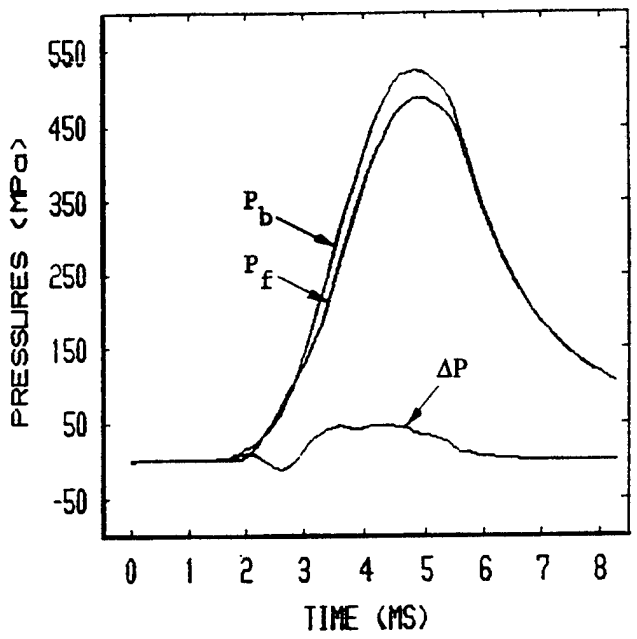

Figure 4. Pressure data for Igniter A.

Igniter B. The pressure-time curves shown in Figure 5 appear to be less smooth in comparison with those shown in Figure 4. The implication is that a perfectly uniform distribution of igniter output over the charge length may not be an ideal arrangement. In reality, as a result of projectile intrusion, the propellant mass in the forward section of the charge is decreasing toward the projectile base. Thus, the ignition stimulus required in the forward section is less than that required in the rear section. The evidence of an early pressure rise in P_f seen in Figure 5 supports this reasoning.

However, there is a noticeable drop in intergranular stress, from 32 MPa for Igniter A to 8 MPa for Igniter B. It should be noted that the resultant muzzle velocity is significantly higher, despite with only a moderate increase in the maximum breech pressure.

Igniter C. With localized ignition near the breech face, the chamber pressures exhibited in Figure 6 are drastically different from those seen previously. Apparently, complex pressure wave motions are taking place between the breech face and the projectile base.

Figure 7 presents a plot of the location of flame front in the gun chamber at various times along with the grain velocity and the intergranular stress at two values of time, 1 ms and 1.7 ms. We note in the figure the intergranular stress first occurs at a location coinciding with the location

Table 2. Summary of Calculated Results

Igniter	W (g)	t_r (ms)	P_b (MPa)	$-\Delta p$ (MPa)	ΔV_m (m/s)	S_i (MPa)	tpmax (ms)	t_{ig} (ms)
Base-line	30	3.0	523	22.2	--	39	4.6	2.0
"	30	1.5	519	45.8	-15	46	3.6	1.2
A	30	3.0	525	12.3	+8	32	4.8	2.2
B	30	3.0	533	13.9	+39	8	5.4	2.7
"	75.5	1.5	518	14.5	+37	7	4.2	1.4
"	30	3.0	532	15.9	+67	7	4.0	1.4
C	30	3.0	507	60.6	-58	45	3.9	1.4
"	30	1.5	501	79.2	-78	48	3.6	1.2
D	30	3.0	525	33.9	+28	35	3.6	1.4
"	30	1.5	524	59.6	+9	42	3.4	1.2
E	30	3.0	541	2.0	+48	26	3.9	1.2
"	30	1.5	537	1.9	+41	27	3.6	0.8
F	30	3.0	529	11.5	+16	13	5.3	2.6
"	75.5	3.0	544	7.5	+46	11	3.8	1.3
G	30	3.0	533	20.2	+41	22	4.6	2.0
"	75.5	3.0	543	25.6	+64	22	3.8	1.2
H	30	3.0	537	0.6	+35	5	5.1	2.3
"	30	1.5	535	1.8	+32	6	3.8	1.1
"	75.5	3.0	551	1.9	+64	6	3.8	1.1

Note:

W = total mass of igniter material; t_r = time period during which igniter output occurs; P_b = maximum pressure at breech; $-\Delta P$ = negative value of $(P_b - P_f)$; ΔV_m = muzzle velocity increase for the igniter over the baseline igniter; S_i = intergranular stress; t_{pmax} = time that the maximum chamber pressure occurs; t_{ig} = time that the flame front reaches the ends of gun chamber.

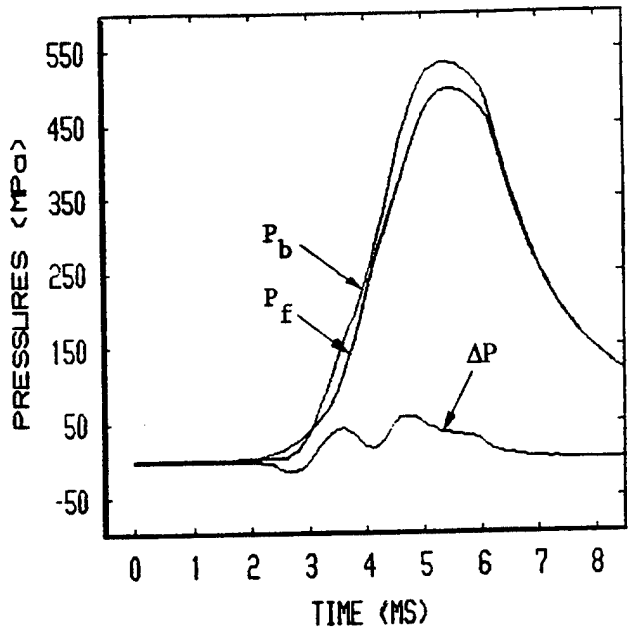

Figure 5. Pressure data for Igniter B.

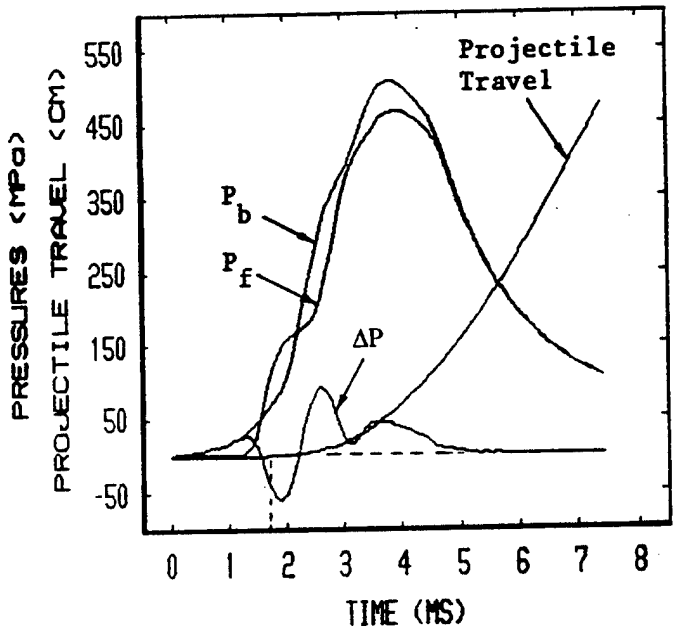

Figure 6. Pressure data and projectile travel for Igniter C.

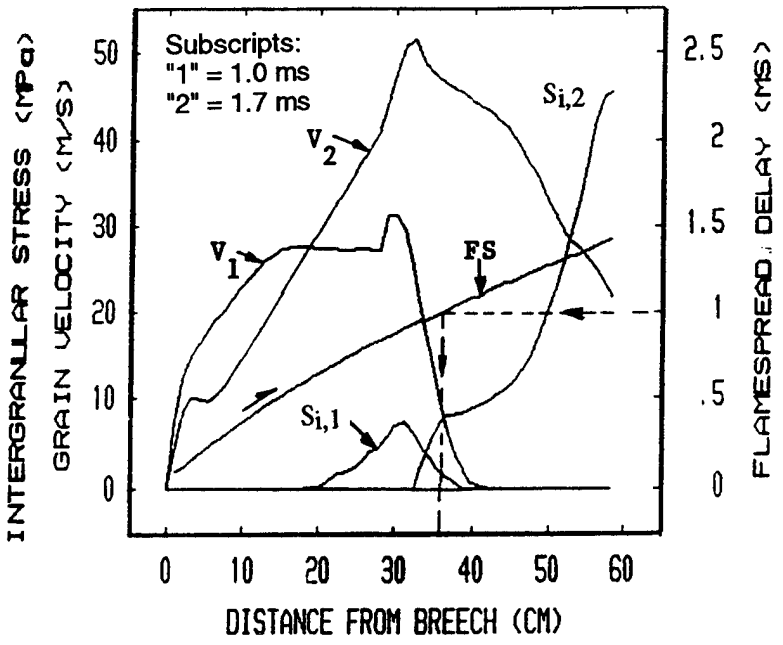

Figure 7. Flamespreading (FS), grain velocity (V), and intergranular stress (S_i) for Igniter C.

where the grain velocity begins decreasing. In fact, this is also the location where propellant compaction begins. Furthermore, from the computer output file, we note that the intergranular stress reaches a maximum at 1.7 ms, which is precisely the instant the projectile begins to move, as indicated in Figure 6. Once the projectile moves, the intergranular stress falls rapidly. A close examination of Figure 7 reveals that the stress wave travels just slightly ahead of the flame front. For example, at 1 ms, the flame is located at 36.5 cm while the stress wave front is 39 cm from the breech face. In the excess of 45 MPa, the stress level could cause severe grain fracture (Lieb 1991) particularly in the region immediately behind the projectile base. When this occurs, local burning surface area of propellant grains will greatly increase. As a consequence, pressure waves will certainly be amplified, and concerns of projectile damage and even a gun failure will arise. It is noted that this igniter has resulted in a large drop in muzzle velocity (58 m/s) in comparison with the baseline round. The drop suggests that the complex wave activities have consumed a large amount of useful energy.

Igniter D. As another example of extreme cases, Figure 8 shows the results from localized ignition initiated at the forward end of the propelling charge. Like the previous case, strong pressure waves exist in the gun chamber. Similar results from forward ignition for other gun systems have recently been obtained at the U.S. Army Research Laboratory. In this case, the flame

spreading and intergranular stress wave are moving toward the breech end. The muzzle velocity is much higher and intergranular stress is much lower than that for Igniter C.

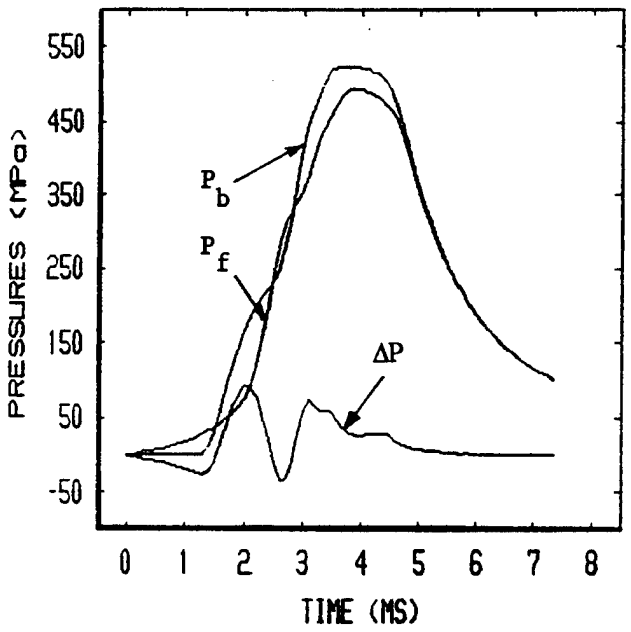

Figure 8. Pressure data for Igniter D.

Igniter E. Figure 9 shows that when ignition is localized at the midsection of the charge, pressure waves disappear completely. Moreover, the muzzle velocity is much higher than the round with baseline igniter.

This ignition process can be understood by examining Figure 10 closely. The flame is first developed at the midsection, and it spreads symmetrically in both directions. Meanwhile, the induced grain motions and intergranular stress waves propagate toward the chamber ends. In the figure, the negative part of the grain velocity results from a direction of grain motion toward the breech end.

Igniter E seems to be ideal for igniting charges with large permeability to gas flow and with no ullage in the propellant bed, especially for stick propelling charges in which many natural flow channels exist. Care should be taken that this may not be suitable for granular charges that have a high loading density, such as those packaged with small grains.

Igniter F. Using this igniter, the chamber pressure profiles exhibited in Figure 11 are also very smooth. The value of -ΔP is small, and the intergranular stress given in Table 2 is only

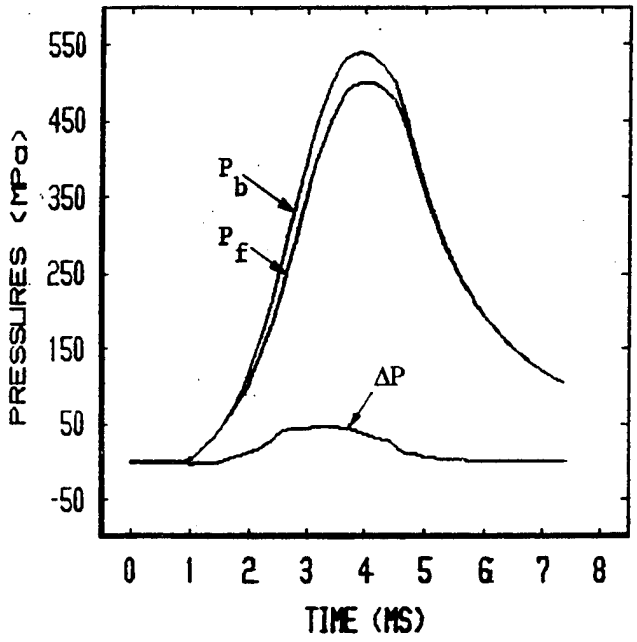

Figure 9. Pressure data for Igniter E.

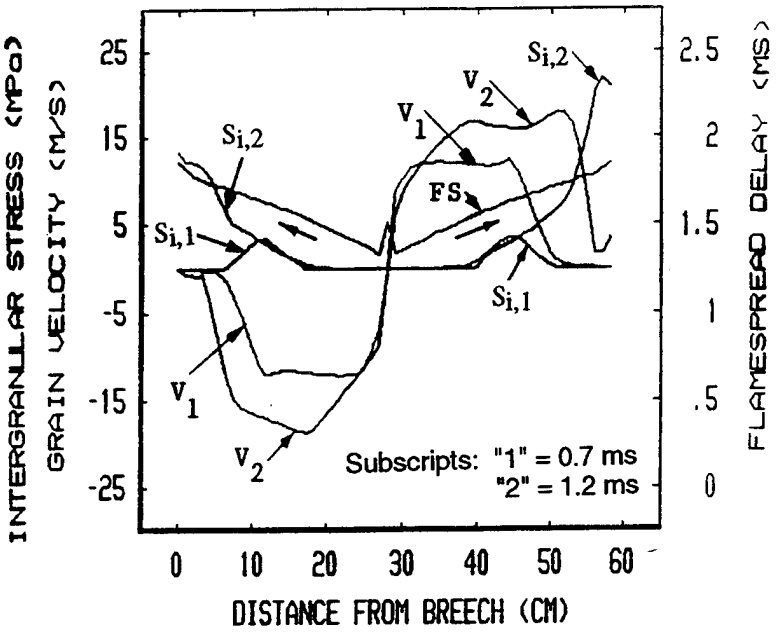

Figure 10. Flamespreading (FS), grain velocity (V), and intergranular stress (S_i) for Igniter E.

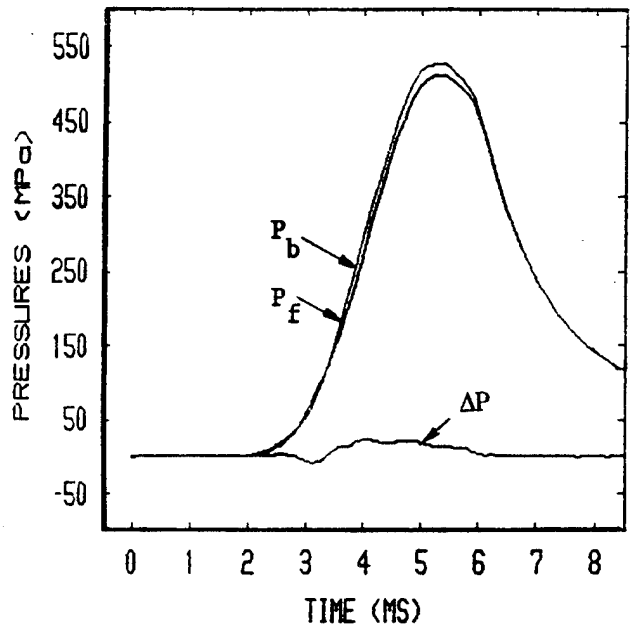

Figure 11. Pressure data for Igniter F.

13 MPa. An increase of igniter output from zero to some value at the forward end of the charge could further improve the ballistic performance.

Igniter G. Using Igniter G, which reverses the output distribution of Igniter F, the pressure behavior shown in Figure 12 becomes undesirable. The resultant intergranular stress increases from 13 MPa to 22 MPa. In addition, the -ΔP doubles, although the muzzle velocity is raised significantly.

Igniter H. Figure 13 presents a graphic representation of the flamespreading in the gun chamber generated by the SiliconGraphics machine. It shows the two flame fronts approaching the two chamber ends. In Figure 14, the two sets of data correspond to two different prescribed output rates for Igniter H, one with a total igniter output of 30 g, the same as all other igniters discussed previously, and the other with 75.5 g. In either case, the pressure curves are very smooth and the value of ΔP is very small on its positive side and almost does not exist on its negative side. Furthermore, the intergranular stress is at the lowest level in all igniters considered, and there is a significant gain in muzzle velocity (see Table 2).

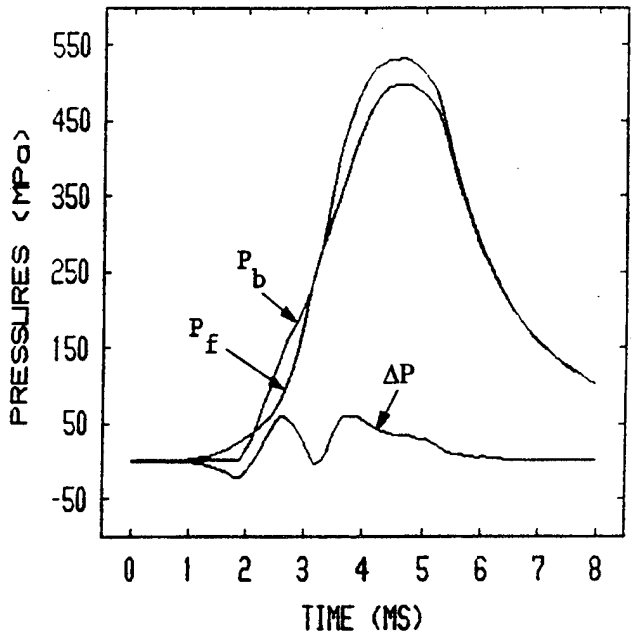

Figure 12. Pressure data for Igniter G.

Projectile Position

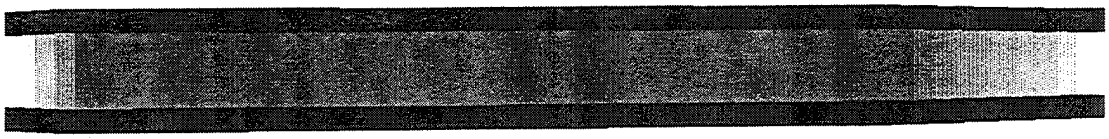

Flamespreading Toward the Two Ends of the Combustion Chamber

Figure 13. Flamespread in gun chamber for Igniter H (at 2 ms)

The ignition delay for Igniter H with 30 g of material appears to be longer than most other igniters. However, it can effectively be reduced by increasing the igniter material while maintaining the same output time (see Figure 14) or by increasing the output rate simply through a reduction of output time as seen in Figure 15.

Igniter H seems to show great promise of ballistic performance for igniting a granular propelling charge.

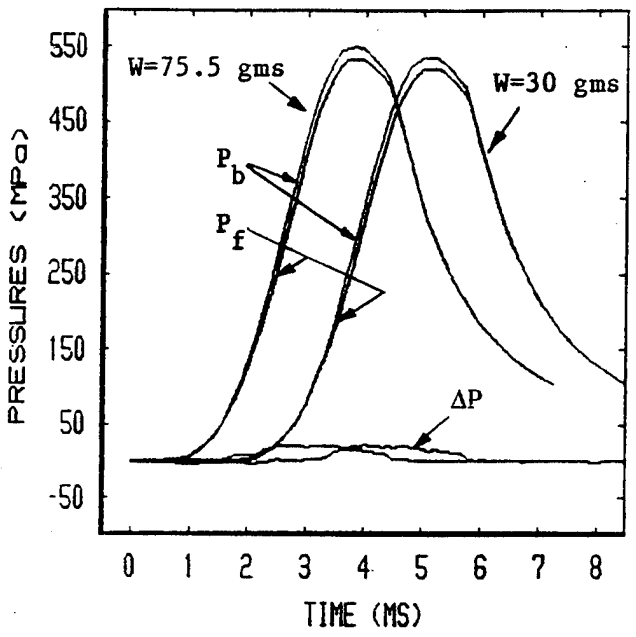

Figure 14 Pressure data for Igniter H (total mass of igniter output = 30 g and 75.5 g).

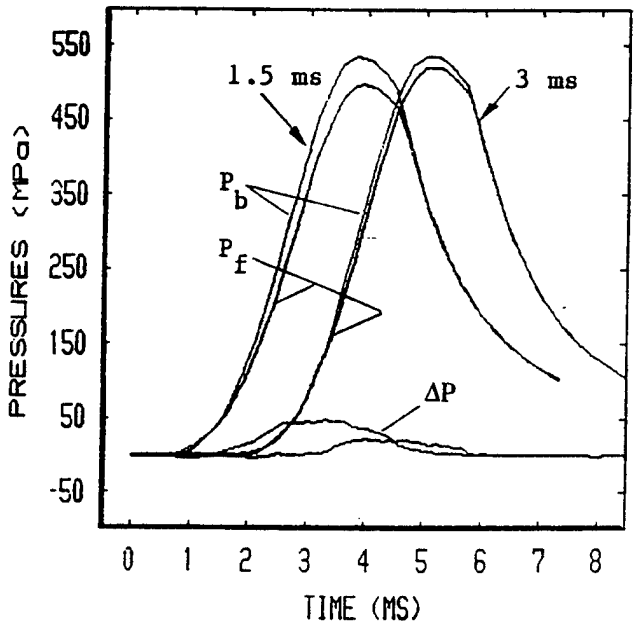

Figure 15. Pressure data for Igniter H (total mass of igniter output = 30 g; total output time = 1.5 ms and 3 ms).

4.3 Effects of Igniter Output Rate.

To examine the effects of igniter output rate, representative calculations are performed for some of the igniters. The output rate is altered in one of two ways: (1) increasing the mass of total igniter material while maintaining the same output time or (2) decreasing the output time while maintaining the same total mass of igniter material. In the first way, the igniter material is increased from 30 g to 75.5 g (see Figure 16b). The mass of 75.5 g is the maximum loading for a fictitious metal primer extending to the forward end of the gun chamber. In the second way, the output time is decreased from 3 ms to 1.5 ms (see Figure 16c), which can be achieved by using fast-burning materials.

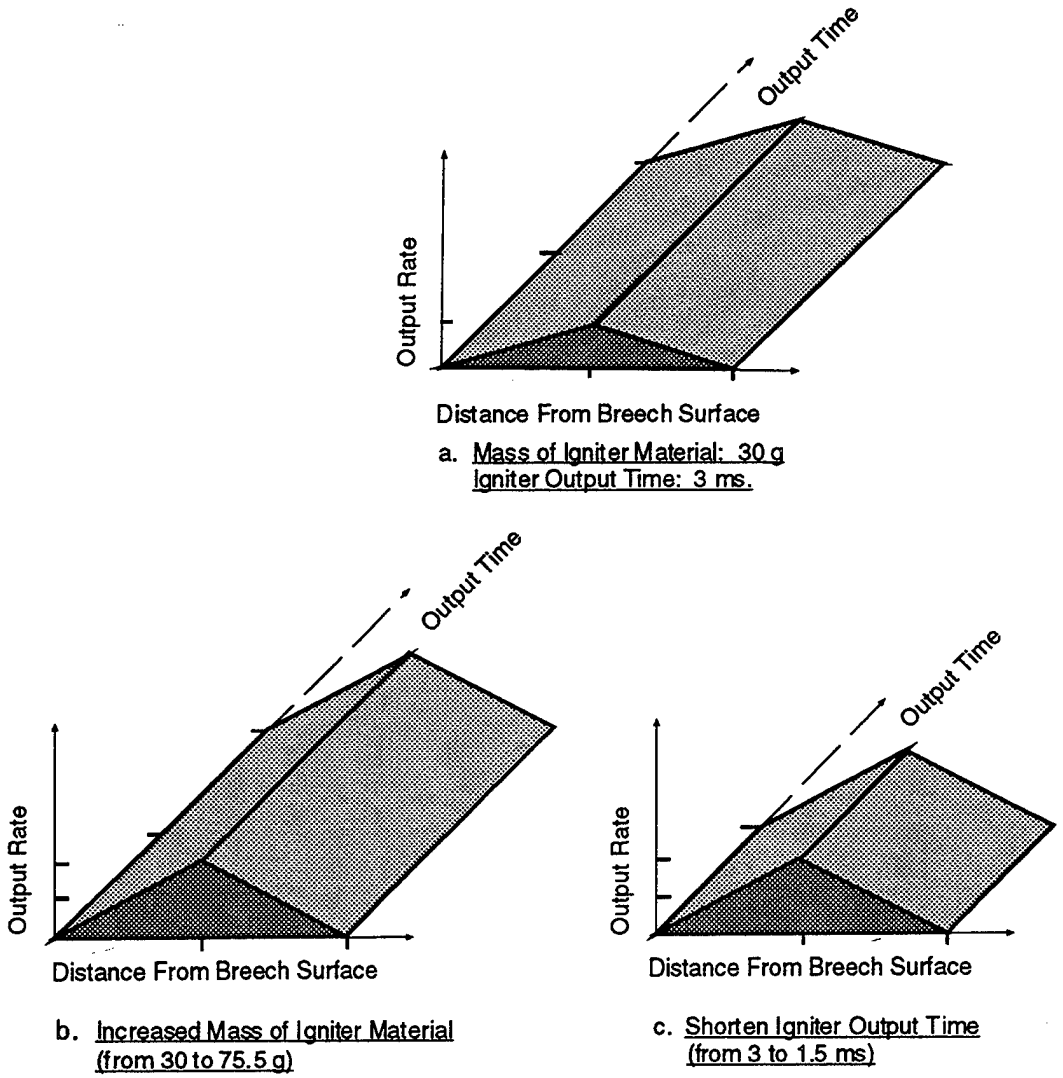

Figure 16. Increased igniter output rate of Igniter H.

Increased Mass of Igniter Material. For the igniters studied (Igniters B, F, G, and H), the results listed in Table 2 show that an increase in igniter mass consistently raises the chamber pressure and the muzzle velocity. The increase also markedly reduces the ignition delay, t_{ig}, and the time at which the maximum breech pressure occurs, t_{pmax}. It does not show any significant detrimental effect on $-\Delta P$ and intergranular stress for these four igniter configurations.

Reduced Igniter Output Time. In all cases studied, the t_{ig} and t_{pmax} are reduced when the output time is shortened. The chamber pressures and muzzle velocity decrease consistently, though the value may be small for some igniters. The magnitude of $-\Delta P$ decreases for Igniter C and D, which generates localized ignition at chamber ends. For Igniters B and H, which provide a uniform or symmetrical distribution of output, the reduction of output time produces little effect on the $-\Delta P$ and the muzzle velocity.

4.4 Correlations of Muzzle Velocity Increase (ΔV_m), Intergranular Stress (S_i), and Maximum Breech Pressure (P_b) With Negative Pressure Difference ($-\Delta P$).

Using the data in Table 2, Figure 17 is plotted for ΔV_m, S_i, and P_b vs. $-\Delta P$. The results in the figure suggest that the values of ΔV_m scatter widely in the range of $-\Delta P$ from 0 to 30 MPa, and ΔV_m decreases as $-\Delta P$ exceeds 30 MPa. As to the intergranular stress S_i, it increases with $-\Delta P$.

With the limited amount of data, the maximum breech pressure, P_b, decreases as $-\Delta P$ increases, and it appears to level off as $-\Delta P$ approaches 60 MPa. In the case that $-\Delta P$ is allowed to increase continuously (in the case of grain fracture), the maximum breech pressure might increase quickly as observed by Horst (1986) in analyzing the firing data from other large-caliber ammunition.

5. CONCLUSIONS

Both igniter output distribution and output rate show strong influences on the ballistic performance of the 105-mm tank granular propellant charge.

Igniter Output Distribution. As observed in the past, those igniters that provide localized output at either end of the granular tank charge result in undesirable high-amplitude pressure waves and high-level intergranular stress. However, an igniter that provides localized ignition at the midsection of the charge will be suitable for charges with large permeability to gas flow. A perfectly uniform distribution of igniter output along the whole length of a granular charge with a

significant projectile intrusion may not necessarily be an ideal arrangement. Igniter H, which provides an output maximum at the midsection of the charge and linearly decreasing to zero at the chamber ends, results in very desirable pressure behavior and muzzle velocity.

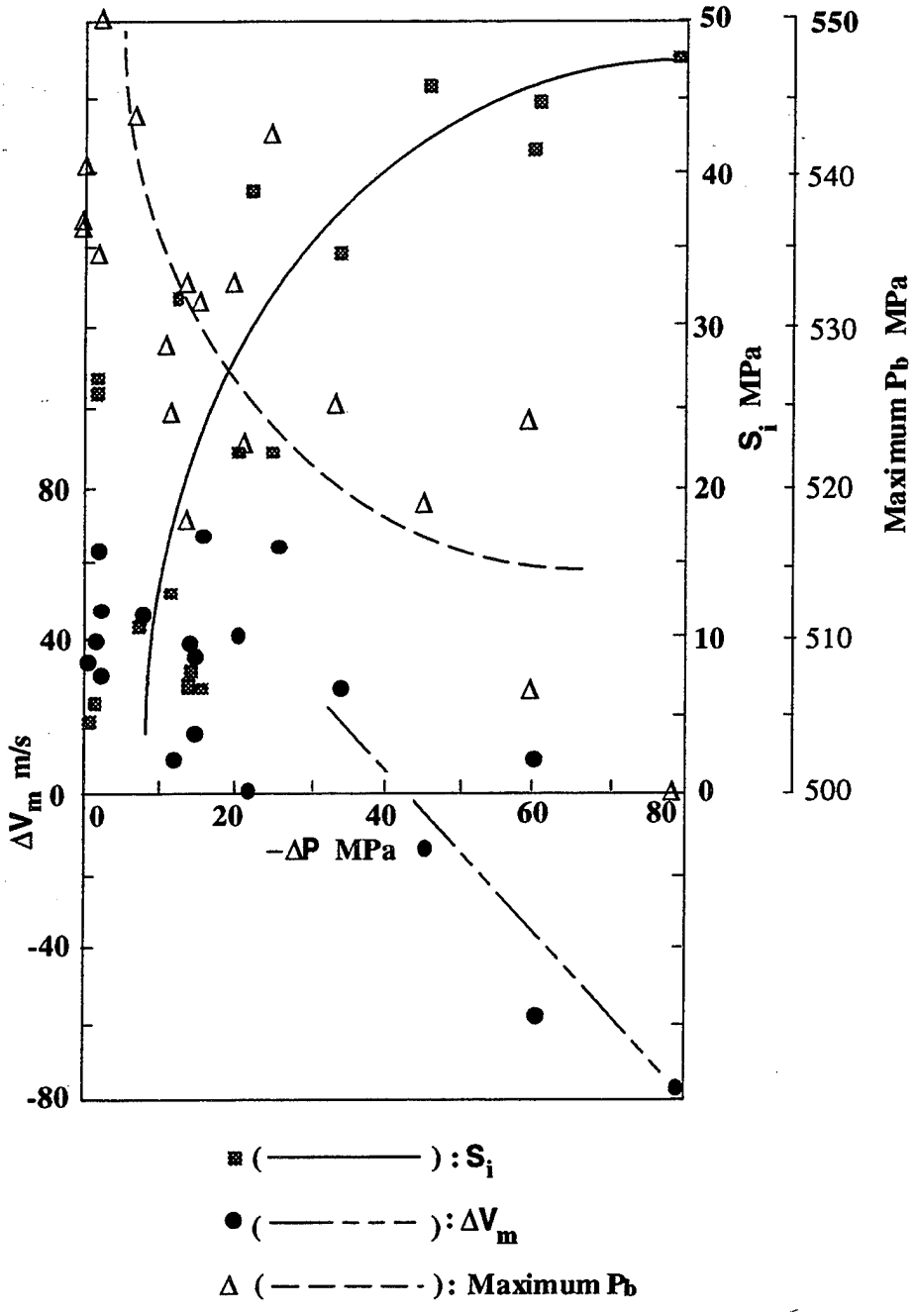

Figure 17. Correlations of muzzle velocity increase (ΔV_m), intergranular stress (S_i), and maximum breech pressure (P_b) with negative pressure difference ($-\Delta P$).

Igniter Output Rate. Variation of igniter output rate may generate various ballistic effects, depending on whether the rate change is accomplished by altering the total mass of igniter material or altering the total output time. In general, an increase in mass will markedly raise the chamber pressure and the muzzle velocity. However, a reduction in the output time while maintaining the same mass may even decrease, though slightly, the chamber pressure and the muzzle velocity. In all cases, an increase in igniter output rate will significantly reduce the ignition delay of the propellant.

The calculated results suggest that the muzzle velocity, V_m, tends to decrease when the negative pressure difference, $-\Delta P$, exceeds approximately 30 MPa. The results also suggest that the intergranular stress, S_i, increases with $-\Delta P$. The maximum breech pressure, P_b, appears to decrease with increasing $-\Delta P$ and to level off as $-\Delta P$ approaches 60 MPa.

INTENTIONALLY LEFT BLANK.

6. REFERENCES

Chang, L. M., and J. J. Rocchio. "Simulator Diagnostics of the Early Phase Ignition Phenomena in a 105-mm Tank Gun Chamber." BRL-TR-2890, U. S. Army Ballistic Research Laboratory, Aberdeen Proving Ground, MD, March 1988.

Gough, P. S. "The XNOVATC Code." BRL-CR-627, U.S. Army Ballistic Research Laboratory, Aberdeen Proving Ground, MD, February 1990.

Horst, A. W. "Breechblow Phenomenology Revisited." BRL-TR-2707, U. S. Army Ballistic Research Laboratory, Aberdeen Proving Ground, MD, January 1986.

Lieb, R. J. "Bed Testing of Gun Propellants at High Strain." CPIA Publication 566, pp. 243, Applied Physics Laboratory, Johns Hopkins University, May 1991.

May, I. W., and A. W. Horst. "Charge Design Considerations and Effect on Pressure Waves in Guns." ARBRL-TR-0227, U.S. Army Ballistic Research Laboratory, December 1978.

Minor, T. C. "Multidimensional Influences on Ignition, Flamespread and Pressurization in Artillery Propelling Charges." CPIA Publication No. 383, pp. 403-414, the 20th JANNAF Combustion Meeting, October 1983.

INTENTIONALLY LEFT BLANK.

NO. OF COPIES	ORGANIZATION
2	ADMINISTRATOR ATTN DTIC DDA DEFENSE TECHNICAL INFO CTR CAMERON STATION ALEXANDRIA VA 22304-6145
1	DIRECTOR ATTN AMSRL OP SD TA US ARMY RESEARCH LAB 2800 POWDER MILL RD ADELPHI MD 20783-1145
3	DIRECTOR ATTN AMSRL OP SD TL US ARMY RESEARCH LAB 2800 POWDER MILL RD ADELPHI MD 20783-1145
1	DIRECTOR ATTN AMSRL OP SD TP US ARMY RESEARCH LAB 2800 POWDER MILL RD ADELPHI MD 20783-1145
	ABERDEEN PROVING GROUND
2	DIR USARL ATTN AMSRL OP AP L (305)

NO. OF COPIES	ORGANIZATION
1	HQDA ATTN SARD TR MS K KOMINOS PENTAGON WASHINGTON DC 20310-0103
1	HQDA ATTN SARD TR DR R CHAIT PENTAGON WASHINGTON DC 20310-0103
1	CHAIRMAN DOD EXPLOSIVES SAFETY BD HOFFMAN BLDG 1 RM 856 C 2461 EISENHOWER AVE ALEXANDRIA VA 22331-0600
1	HQS US ARMY MATERIEL CMD ATTN AMCICP AD M FISETTE 5001 EISENHOWER AVE ALEXANDRIA VA 22333-0001
1	US ARMY BMDS CMD ADVANCED TECHLGY CTR PO BOX 1500 HUNTSVILLE AL 35807-3801
2	PM ADV FIELD ARTLRY SYSTEM ATTN SFAE ASM AF E LTC A ELLIS T KURIATA PICATINNY ARSENAL NJ 07806-5000
1	PM ADV FIELD ARTLRY SYSTEM ATTN SFAE ASM AF Q W WARREN PICATINNY ARSENAL NJ 07806-5000
1	CDR US ARMY ARDEC PROD BASE MODERNIZATION AGENCY ATTN AMSMC PBM A SIKLOSI PICATINNY ARSENAL NJ 07806-5000
1	CDR US ARMY ARDEC PROD BASE MODERNIZATION AGENCY ATTN AMSMC PBM E L LAIBSON PICATINNY ARSENAL NJ 07806-5000

NO. OF COPIES	ORGANIZATION
1	PM PEO ARMAMENTS TANK MAIN ARMAMENT SYSTEM ATTN AMCPM TMA PICATINNY ARSENAL NJ 07806-5000
1	PM PEO ARMAMENTS TANK MAIN ARMAMENT SYSTEM ATTN AMCPM TMA 105 PICATINNY ARSENAL NJ 07806-5000
1	PM PEO ARMAMENTS TANK MAIN ARMAMENT SYSTEM ATTN AMCPM TMA 120 PICATINNY ARSENAL NJ 07806-5000
1	PM PEO ARMAMENTS TANK MAIN ARMAMENT SYSTEM ATTN AMCPM TMA AS H YUEN PICATINNY ARSENAL NJ 07806-5000
2	CDR US ARMY ARDEC ATTN AMSTA AR CCH V C MANDALA E FENNELL PICATINNY ARSENAL NJ 07806-5000
1	CDR US ARMY ARDEC ATTN AMSTA AR CCH T L ROSENDORF PICATINNY ARSENAL NJ 07806-5000
1	CDR US ARMY ARDEC ATTN AMSTA AR CCS PICATINNY ARSENAL NJ 07806-5000
1	CDR US ARMY ARDEC ATTN AMSTA AR AEE J LANNON PICATINNY ARSENAL NJ 07806-5000
1	COMMANDER US ARMY ARDEC ATTN AMSTA AR AES S KAPLOWITZ PICATINNY ARSENAL NJ 07806-5000

NO. OF COPIES	ORGANIZATION
8	CDR US ARMY ARDEC ATTN AMSTA AR AEE B D DOWNS S EINSTEIN S WESTLEY S BERNSTEIN J RUTKOWSKI P O'REILLY R CIRINCIONE P HUI PICATINNY ARSENAL NJ 07806-5000
2	COMMANDER US ARMY ARDEC ATTN AMSTA AR AEE W M MEZGER P LU PICATINNY ARSENAL NJ 07806-5000
2	US ARMY RESEARCH OFFICE ATTN TECHNICAL LIBRARY D MANN PO BOX 12211 RESEARCH TRIANGLE PARK NC 27709-2211
1	CDR USACECOM R&D TECHNICAL LIBRARY ATTN ASQNC ELC IS L R MYER CTR FORT MONMOUTH NJ 07703-5301
1	PM US TANK AUTOMOTIVE CMD ATTN AMCPM ABMS T DEAN WARREN MI 48092-2498
1	PM US TANK AUTOMOTIVE CMD FIGHTING VEHICLE SYSTEMS ATTN SFAE ASM BV WARREN MI 48397-5000
1	PM ABRAMS TANK SYSTEM ATTN SFAE ASM AB WARREN MI 48397-5000
1	DIR HQ TRAC RPD ATTN ATCD MA FORT MONROE VA 23651-5143

NO. OF COPIES	ORGANIZATION
1	COMMANDANT US ARMY COMMAND & GEN STAFF COLLEGE FT LEAVENWORTH KS 66027
1	COMMANDER RADFORD ARMY AMMO PLANT ATTN SMCAR QA HI LIB RADFORD VA 24141-0298
1	COMMANDER US ARMY NGIC ATTN AMXST MC 3 220 SEVENTH STREET NE CHARLOTTESVILLE VA 22901-5396
1	COMMANDANT US ARMY FIELD ARTLRY CTR & SCHOOL ATTN ATSF CD COL T STRICKLIN FT SILL OK 73503-5600
1	COMMANDANT US ARMY FIELD ARTLRY CTR & SCHOOL ATTN ATSF CN P GROSS FT SILL OK 73503-5600
1	CMDT US ARMY ARMOR SCHOOL ARMOR AGENCY ATTN ATZK CD MS M FALKOVITCH FORT KNOX KY 40121-5215
1	CDR NAVAL RSRCH LAB ATTN TECHNICAL LIBRARY CODE 4410 WASHINGTON DC 20375-5000
1	COMMANDER NAVAL SURFACE WARFARE CTR ATTN CODE 730 SILVER SPRING MD 20903-5000

NO. OF COPIES	ORGANIZATION
1	COMMANDER NAVAL SURFACE WARFARE CTR ATTN CODE R 13 R BERNECKER SILVER SPRING MD 20903-5000
5	COMMANDER NAVAL SURFACE WARFARE CTR ATTN T C SMITH K RICE S MITCHELL S PETERS TECHNICAL LIBRARY INDIAN HEAD MD 20640-5000
1	COMMANDER NAVAL SURFACE WARFARE CTR ATTN CODE G30 GUNS & MUNITIONS DIV DAHLGREN VA 22448-5000
1	COMMANDER NAVAL SURFACE WARFARE CTR ATTN CODE G33 T DORAN DAHLGREN VA 22448-5000
1	COMMANDER NAVAL SURFACE WARFARE CTR ATTN CODE E23 TECHNICAL LIBRARY DAHLGREN VA 22448-5000
1	COMMANDER NAVAL AIR WARFARE CTR INFORMATION SCIENCE DIV CHINA LAKE CA 93555-6001
1	COMMANDING OFFICER NAVAL UNDERWATER SYSTEMS CTR ATTN CODE 5B331 TECH LIBRARY NEWPORT RI 02840
1	CNTRL INTELLIGENCE AGNCY OFC OF THE CNTRL RFRNCES DISSEMINATION BRANCH ROOM GE 47 HQS WASHINGTON DC 20502

NO. OF COPIES	ORGANIZATION
1	CNTRL INTELLIGENCE AGNCY ATTN J BACKOFEN NHB ROOM 5N01 WASHINGTON DC 20505
1	DIR SANDIA NATL LABS ATTN 8741 G A BENEDITTI PO BOX 969 LIVERMORE CA 94551-0969
1	DIR LOS ALAMOS NATIONAL LAB ATTN T3 D BUTLER PO BOX 1663 LOS ALAMOS NM 87544
1	DIR LOS ALAMOS NATL LAB ATTN M DIVISION B CRAIG PO BOX 1663 LOS ALAMOS NM 87544
2	BATTELLE ATTN TWSTIAC V LEVIN 505 KING AVE COLUMBUS OH 43201-2693
1	BATTELLE PNL ATTN MR MARK GARNICH PO BOX 999 RICHLAND WA 99352
2	PENNSYLVANIA STATE UNIV DEPT OF MECH ENGRNG ATTN V YANG K KUO UNIVERSITY P[ARK PA 16802-7501
2	CPIA JHU ATTN H J HOFFMAN T CHRISTIAN 10630 LITTLE PATUXENT PKY SUITE 202 COLUMBIA MD 21044-3200
2	AAI CORPORATION ATTN J FRANKLE D CLEVELAND PO BOX 126 HUNT VALLEY MD 21030-0126

NO. OF COPIES	ORGANIZATION
6	ALLIANT TECHSYSTEMS INC ATTN R E TOMPKINS J KENNEDY J BODE C CANDLAND L OSGOOD R BURETTA 600 SECOND ST NE HOPKINS MN 55343
1	IITRI ATTN M J KLEIN 10 W 35TH STREET CHICAGO IL 60616-3799
3	HERCULES INC ATTN D A WORRELL W J WORRELL C CHANDLER RADFORD ARMY AMMO PLANT RADFORD VA 24141-0299
2	HERCULES INC ATTN WILLIAM B WALKUP THOMAS F FARABAUGH ALLEGHENY BALLISTICS LAB PO BOX 210 ROCKET CENTER WV 26726
1	HERCULES INC ATTN B M RIGGLEMAN HERCULES PLAZA WILMINGTON DE 19894
3	OLIN ORDNANCE ATTN E J KIRSCHKE A F GONZALEZ D W WORTHINGTON PO BOX 222 ST MARKS FL 32355-0222
1	OLIN ORDNANCE ATTN H A MCELROY 10101 9TH STREET NORTH ST PETERSBURG FL 33716
1	PAUL GOUGH ASSOC INC ATTN P S GOUGH 1048 SOUTH ST PORTSMOUTH NH 03801-5423

NO. OF COPIES	ORGANIZATION
1	PHYSICS INTRNTNL LIBRARY ATTN H WAYNE WAMPLER PO BOX 5010 SAN LEANDRO CA 94577-0599
1	PRINCETON CMBSTN RSRCH LABS INC ATTN N A MESSINA PRINCETON CORPORATE PLAZA 11 DEERPARK DR BLDG IV SUITE 119 MONMOUTH JUNCTION NJ 08852
1	SAIC ATTN M PALMER 2109 AIR PARK RD ALBUQUERQUE NM 87106
1	SOUTHWEST RSRCH INSTITUTE ATTN J P RIEGEL 6220 CULEBRA ROAD SAN ANTONIO TX 78228-0510
3	THIOKOL CORPORATION ATTN R WILLER R BIDDLE TECH LIBRARY ELKTON DIVISION PO BOX 241 ELKTON MD 21921-0241
3	VERITAY TECHLGY INC ATTN E FISHER A CRICKENBERGER J BARNES 4845 MILLERSPORT HWY EAST AMHERST NY 14501-0305
1	SRI INTERNATIONAL ATTN TECH LIBRARY PROPULSION SCIENCES DIV 333 RAVENWOOD AVE MENLO PARK CA 94025-3493

NO. OF COPIES	ORGANIZATION
	ABERDEEN PROVING GROUND
1	CDR USACSTA ATTN STECS LI R HENDRICKSEN
29	DIR USARL ATTN AMSRL WT P A HORST AMSRL WT PA T MINOR T COFFEE G WREN A BIRK J DE SPIRITO A JUHASZ J KNAPTON C RUTH K WHITE L-M CHANG (5 CP) J COLBURN P CONROY G KELLER D KOOKER M NUSCA T ROSENBERGER AMSRL WT PB E SCHMIDT M BUNDY B GUIDOS AMSRL WT PC R FIFER J VANDERHOFF R BEYER M MILLER AMSRL WT PD B BURNS

USER EVALUATION SHEET/CHANGE OF ADDRESS

This Laboratory undertakes a continuing effort to improve the quality of the reports it publishes. Your comments/answers to the items/questions below will aid us in our efforts.

1. ARL Report Number/Author ARL-TR-1092 (Chang) Date of Report May 1996

2. Date Report Received _____

3. Does this report satisfy a need? (Comment on purpose, related project, or other area of interest for which the report will be used.) _____

4. Specifically, how is the report being used? (Information source, design data, procedure, source of ideas, etc.) _____

5. Has the information in this report led to any quantitative savings as far as man-hours or dollars saved, operating costs avoided, or efficiencies achieved, etc? If so, please elaborate. _____

6. General Comments. What do you think should be changed to improve future reports? (Indicate changes to organization, technical content, format, etc.) _____

CURRENT ADDRESS

_____
Organization

_____
Name

_____
Street or P.O. Box No.

_____
City, State, Zip Code

7. If indicating a Change of Address or Address Correction, please provide the Current or Correct address above and the Old or Incorrect address below.

OLD ADDRESS

_____
Organization

_____
Name

_____
Street or P.O. Box No.

_____
City, State, Zip Code

(Remove this sheet, fold as indicated, tape closed, and mail.)
(DO NOT STAPLE)

DEPARTMENT OF THE ARMY

OFFICIAL BUSINESS

NO POSTAGE
NECESSARY
IF MAILED
IN THE
UNITED STATES

BUSINESS REPLY MAIL
FIRST CLASS PERMIT NO 0001,APG,MD

POSTAGE WILL BE PAID BY ADDRESSEE

DIRECTOR
U.S. ARMY RESEARCH LABORATORY
ATTN: AMSRL-WT-PA
ABERDEEN PROVING GROUND, MD 21005-5066